Dicyanoaurate-Based Heterobimetallic Uranyl Coordination Polymers

Electronic Supplementary Information

Matthew L. Brown, Jeffrey S. Ovens, and Daniel B. Leznoff*

Table S1 Crystallographic Data For Peroxo-Containing Compounds **1a**, **1b** and **1c**

Compound reference	**1a**	**1b**	**1c**
Chemical formula	$C_{36}H_{72}Au_2N_8O_{12}U_2$	$C_{36}H_{72}Au_2N_8O_{12}U_2$	$C_{36}H_{74}Au_2N_6O_6U_2$
FW ($g\,mol^{-1}$)	1678.99	1678.99	1135.61
Crystal system	monoclinic	triclinic	triclinic
Space group	$P2_1/n$	$P\bar{1}$	$P\bar{1}$
Radiation Used	MoKα	MoKα	MoKα
a (Å)	11.1927(18)	11.231(2)	11.1439(5)
b (Å)	32.757(6)	15.587(3)	12.7533(6)
c (Å)	14.629(2)	29.978(6)	15.0713(8)
α (°)	90	88.081(5)	69.826(2)
β (°)	94.481(4)	86.958(5)	77.625(2)
γ (°)	90	89.110(5)	84.510(2)
V (Å^3)	5347.2(15)	5236.9(17)	1963.28(17)
Z	4	4	2
T (K)	150(2)	150(2)	150(2)
μ (mm^{-1})	11.565	11.809	7.981
Reflns. all	43489	18412	12930
Reflns. unique	13816	18412	12930
Goodness of fit	0.997	1.079	1.025
$[I_0 \geq 2\sigma\ (I_0)]^{\alpha}$			
R_1	0.0602	0.0842	0.0392
wR_2	0.0847	0.1752	0.0709
(all data)			
R_1	0.1387	0.1536	0.0722
wR_2	0.1017	0.2004	0.0847

$^{\alpha}$ Function minimized: $\sum w(F_o^2 - F_c^2)^2$, $R_1 = \sum ||F_o| - |F_c|| \div \sum |F_o|$,
$wR_2 = \sqrt{\sum w(F_o^2 - F_c^2)^2 \div \sum wF_o^2}$, $w = [\sigma^2(F_o^2) + (aP)^2 + bP]^{-1}$, $P = (F_o^2 + 2F_c^2) \div 3$

Table S2 Crystallographic Data For Compounds **2a**, **2b** and **3**

Compound reference	**2a**	**2b**	**3**
Chemical formula	$C_{38}H_{30}AuN_5O_8P_2U$	$C_{38}H_{30}AuN_5O_8P_2U$	$C_{76}H_{60}Au_2N_8O_8P_4U$
FW ($g\,mol^{-1}$)	1181.62	1181.62	1969.20
Crystal system	triclinic	triclinic	triclinic
Space group	$P\bar{1}$	$P\bar{1}$	$P\bar{1}$
Radiation Used	CuKα	CuKα	MoKα
a (Å)	11.8363(3)	9.2421(3)	10.7013(6)
b (Å)	12.6558(3)	10.8293(3)	13.3921(8)
c (Å)	14.7514(4)	11.1451(2)	14.0367(9)
α (°)	99.118(2)	100.608(2)	113.946(3)
β (°)	110.205(2)	90.338(2)	101.917(3)
γ (°)	92.652(2)	114.663(2)	93.446(3)
V (Å^3)	2035.34(9)	992.10(5)	1775.42(19)
Z	2	1	1
T (K)	rt$^{\beta}$	rt$^{\beta}$	150(2)
μ (mm^{-1})	19.003	19.493	6.549
Reflns. all	52146	15618	78011
Reflns. unique	3627	3487	8816
Goodness of fit	1.060	1.036	1.031
$[I_0 \geq 2\sigma\ (I_0)]^{\alpha}$			
R_1	0.0302	0.0337	0.0248
wR_2	0.0738	0.0708	0.0413
(all data)			
R_1	0.0385	0.0585	0.0413
wR_2	0.0794	0.0800	0.0602

$^{\alpha}$ Function minimized: $\sum w(F_o^2 - F_c^2)^2$, $R_1 = \sum ||F_o| - |F_c|| \div \sum |F_o|$,
$wR_2 = \sqrt{\sum w(F_o^2 - F_c^2)^2 \div \sum wF_o^2}$, $w = [\sigma^2(F_o^2) + (aP)^2 + bP]^{-1}$, $P = (F_o^2 + 2F_c^2) \div 3$

$^{\beta}$ Room temperature approximated to 298.15 K.
The actual temperature of the room in question was most likely between 288 K to 293 K.

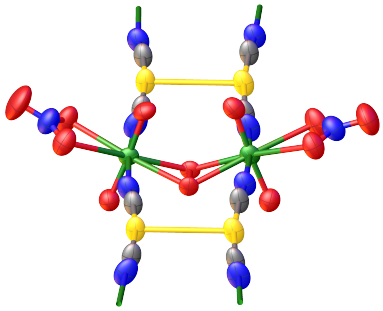

Fig. S1 Divergence of C—Au—C angle from 180° in **1a**, along with the U—O_2—U bond angle. Ellipsoid colours: U, Green; O, red; N, blue; C, grey; Au, gold.

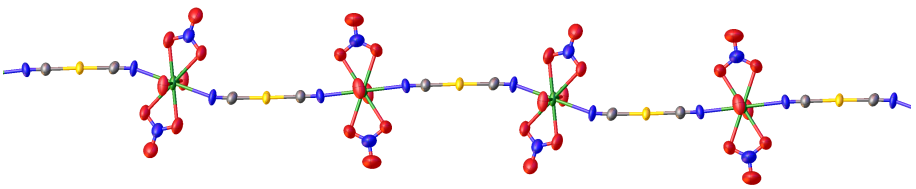

Fig. S2 One-dimensional chain structure of **2a**.

Table S3 Crystallographic Data for Chelating Ancillary Ligand Containing Compounds **4**, **5** and **6**

Compound reference	**4**	**5**	**6**
Chemical formula	$C_{28}H_{30}N_8Au_2O_8U_2$	$C_{28}H_{26}Au_2N_8O_6U_2$	$C_{36}H_{23}AuN_{10}O_8U_2$
FW ($g\,mol^{-1}$)	1476.58	1440.55	1396.65
Crystal system	triclinic	monoclinic	monoclinic
Space group	$P\bar{1}$	$P2_1/n$	$C2/c$
Radiation Used	MoKα	MoKα	CuKα
a (Å)	6.1056(9)	12.4180(4)	12.2358(7)
b (Å)	12.5052(18)	11.3951(3)	24.0833(18)
c (Å)	13.1277(19)	12.7018(4)	14.6019(9)
α (°)	113.603(4)	90	90
β (°)	97.039(4)	109.867(2)	112.146(5)
γ (°)	99.801(4)	90	90
V (Å^3)	884.6(2)	1690.39(9)	3985.4(5)
Z	1	2	2
T (K)	150(2)	150(2)	150(2)
μ (mm^{-1})	17.448	18.255	29.958
Reflns. all		12519	12620
Reflns. unique		12519	3627
Goodness of fit	1.042	1.062	0.996
$[I_0 \geq 2\sigma\ (I_0)]^\alpha$			
R_1	0.0488	0.0561	0.0409
wR_2	0.0769	0.1405	0.0947
(all data)			
R_1	0.0806	0.0975	0.0566
wR_2	0.0833	0.1634	0.1015

$^\alpha$ Function minimized: $\sum w(F_o^2 - F_c^2)^2$, $R_1 = \sum ||F_o| - |F_c|| \div \sum |F_o|$,
$wR_2 = \sqrt{\sum w(F_o^2 - F_c^2)^2 \div \sum wF_o^2}$, $w = [\sigma^2(F_o^2) + (aP)^2 + bP]^{-1}$, $P = (F_o^2 + 2F_c^2) \div 3$

Table S4 U=O bond lengths.

Compound	U=O (Å)	Compound	U=O (Å)
1a	1.742(6)	**2a**	1.739(5)
	1.749(7)		1.721(5)
	1.753(7)		
	1.765(7)	**2b**	1.745(6)
1b	1.748(17)	**3**	1.754(2)
	1.750(17)		
	1.764(19)		
	1.775(19)	**4**	1.748(8)
	1.734(19)		1.745(8)
	1.767(18)		
	1.761(19)	**5**	1.762(7)
	1.780(19)		1.772(6)
1c	1.85(2)	**6**	1.789(8)
	1.72(2)		1.789(7)
	1.847(17)		
	1.68(2)		

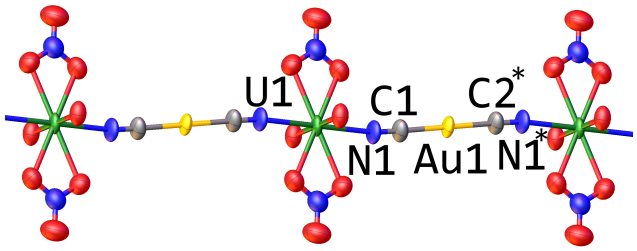

Fig. S3 One-dimensional chain structure of $[PPN][UO_2(NO_3)_2Au(CN)_2]$ (**2b**). $[PPN]^+$ counterions omitted for clarity. Green ellipsoids represent uranium, red: oxygen, blue: nitrogen, grey: carbon, gold: gold.

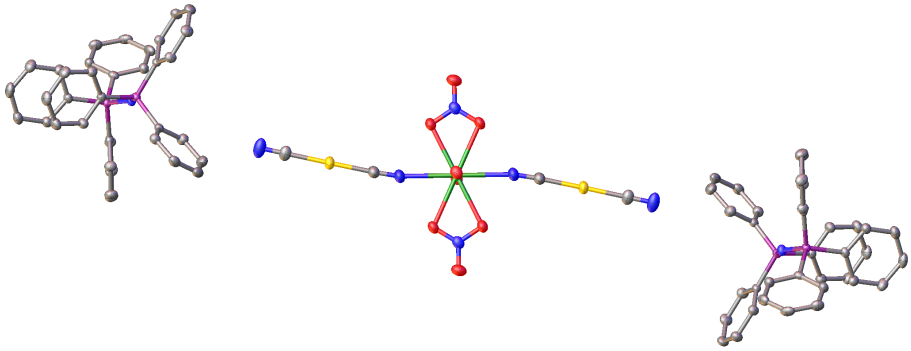

Fig. S4 Structure of $[PPN][UO_2(NO_3)_2(Au(CN)_2)_2]$ (**3**): Instead of binding to a uranium atom as in **2a** and **2b** and creating a coordination polymer the cyano groups are oriented towards the counterion. Ellipsoid colours: U, Green; O, red; N, blue; C, grey; Au, gold.

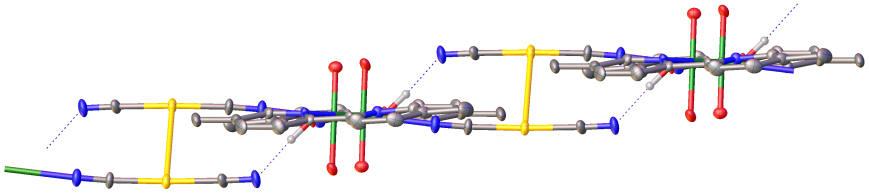

Fig. S5 The hydrogen and aurophilic bonding in **5** gives rise to propagation that is not in-plane with the equatorial plane of the uranyl centres. Ellipsoid colours: U, Green; O, red; N, blue; C, grey; Au, gold.

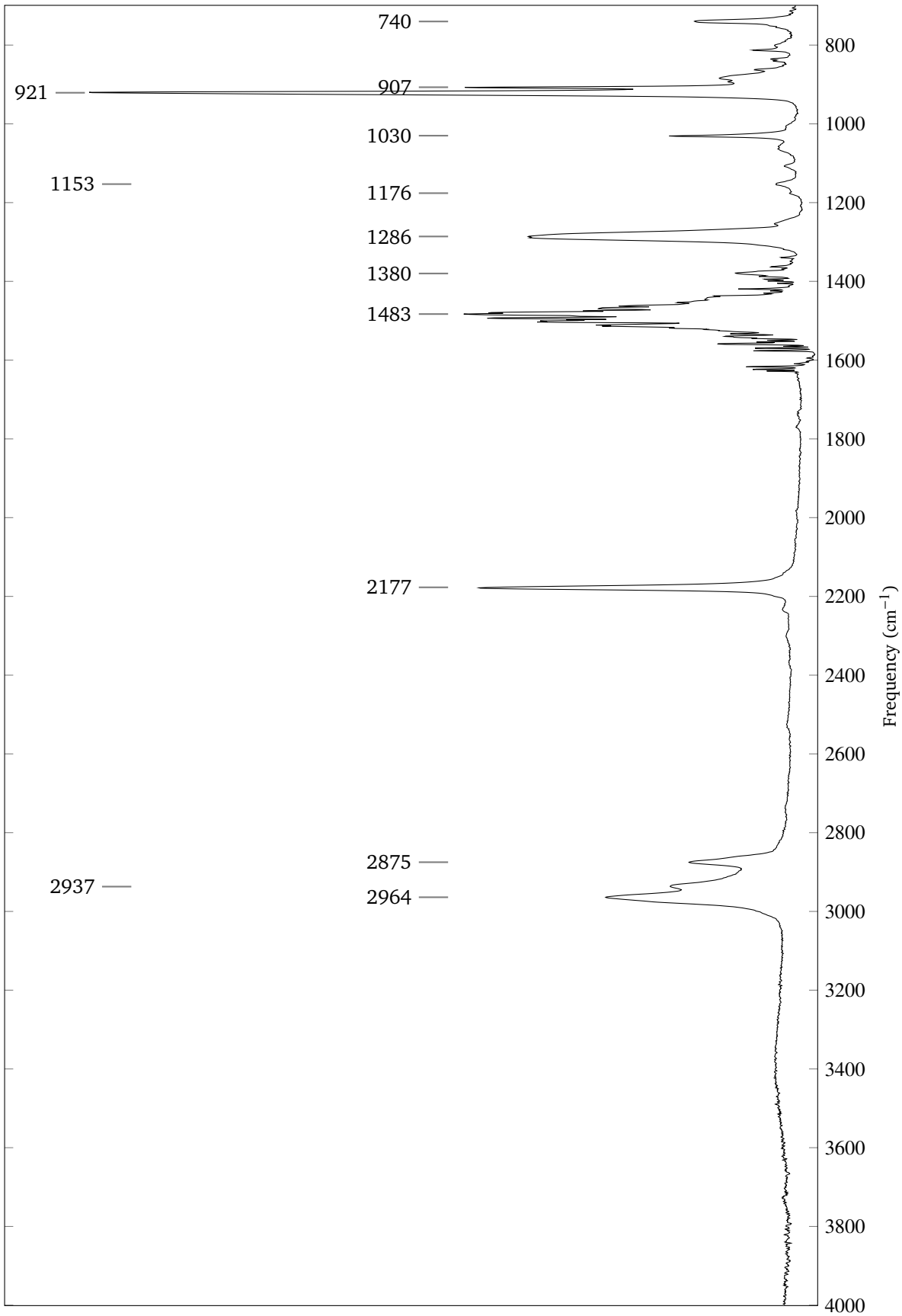

Figure S6: IR Spectrum of Methanol Polymorph of Peroxo-Bridged Coordination Polymer **1a** With Selected Peaks

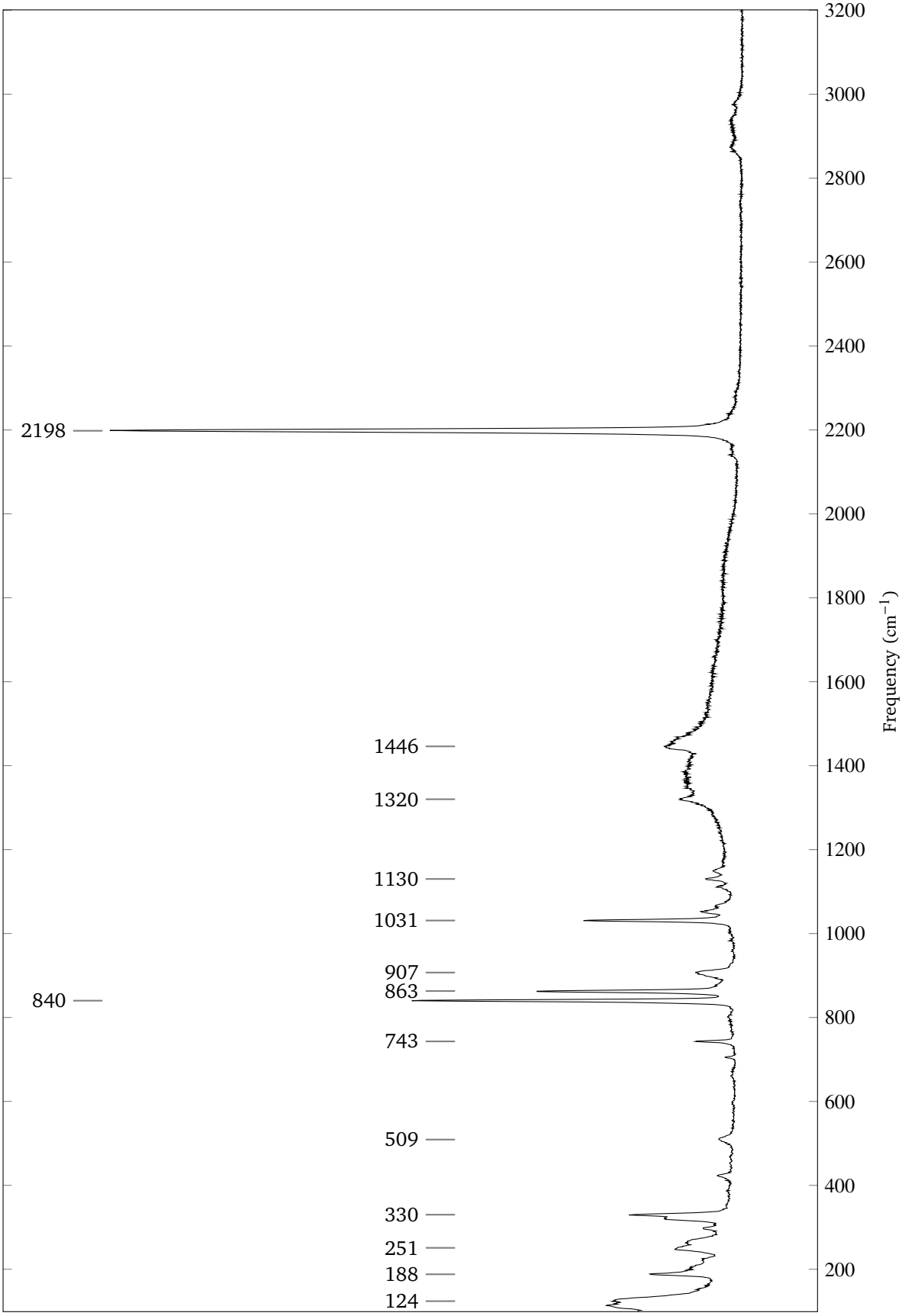

Figure S7: Raman Spectrum of Methanol Polymorph of Peroxo-Bridged Coordination Polymer **1a** With Selected Peaks

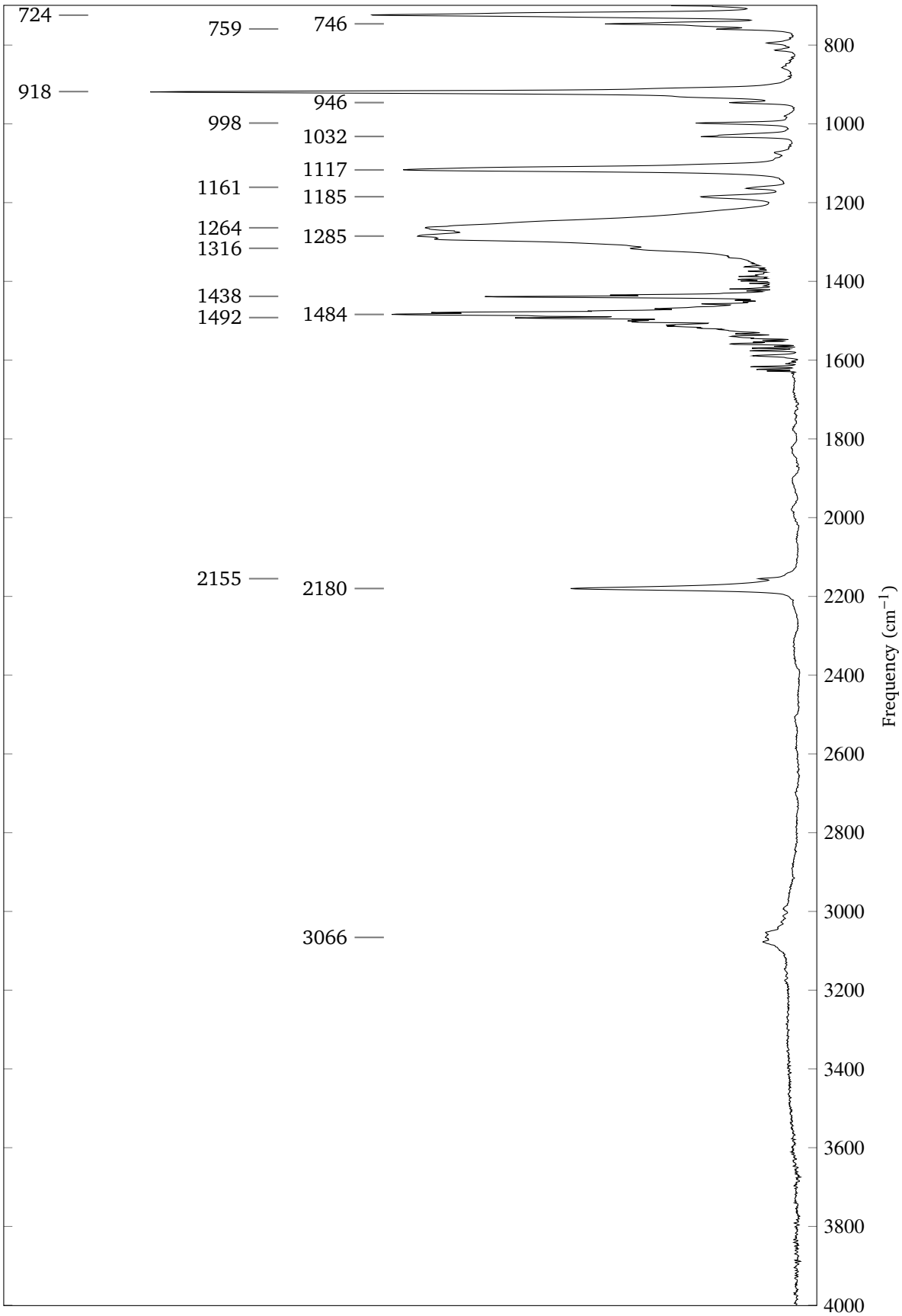

Figure S8: IR Spectrum of $[PPN]^+$-Salt of Peroxo-Bridged Coordination Polymer **1c** With Selected Peaks

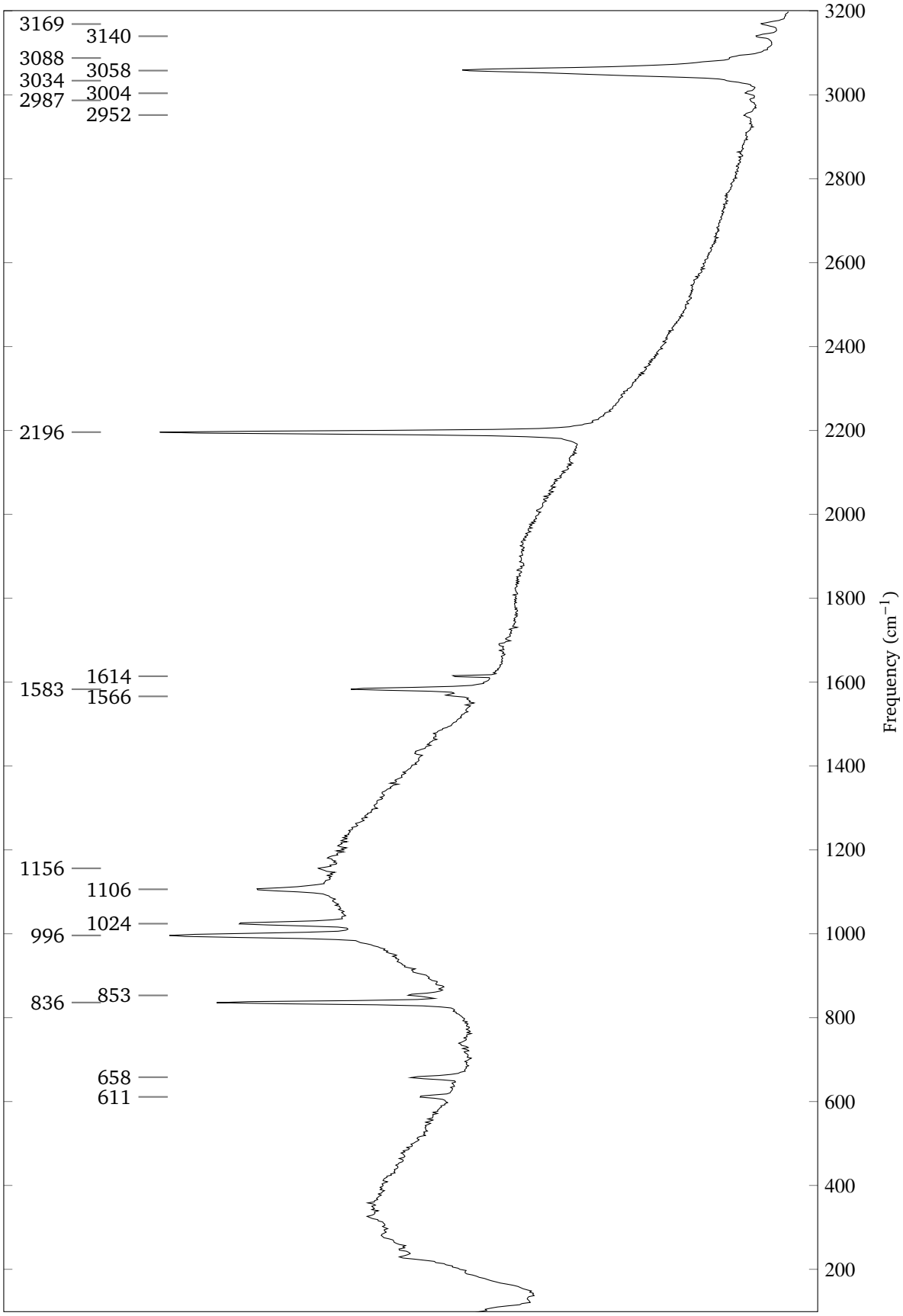

Figure S9: Raman Spectrum of $[PPN]^+$-Salt of Peroxo-Bridged Coordination Polymer **1c** With Selected Peaks

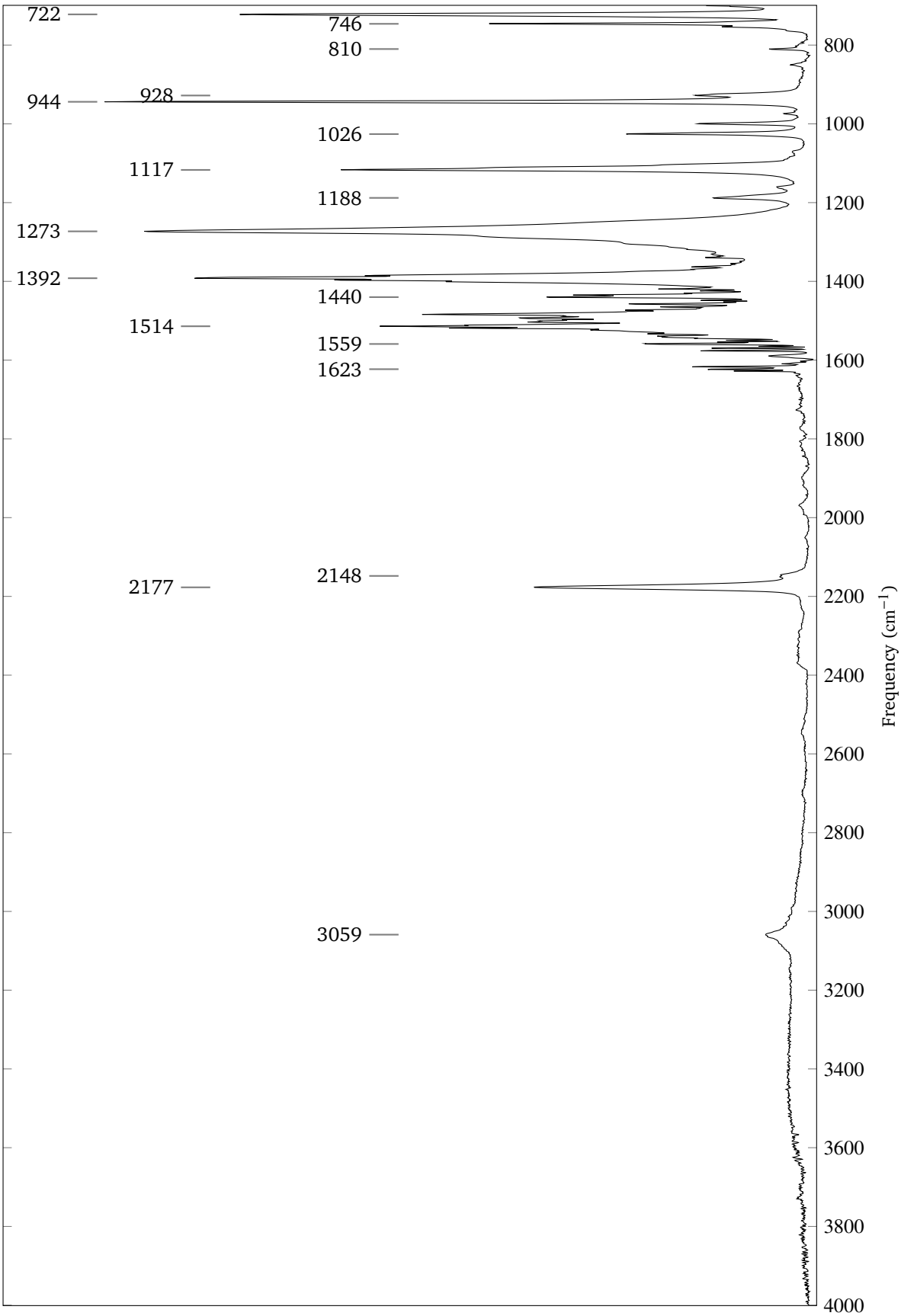

Figure S10: IR Spectrum of Coordination Polymer **2** With Selected Peaks

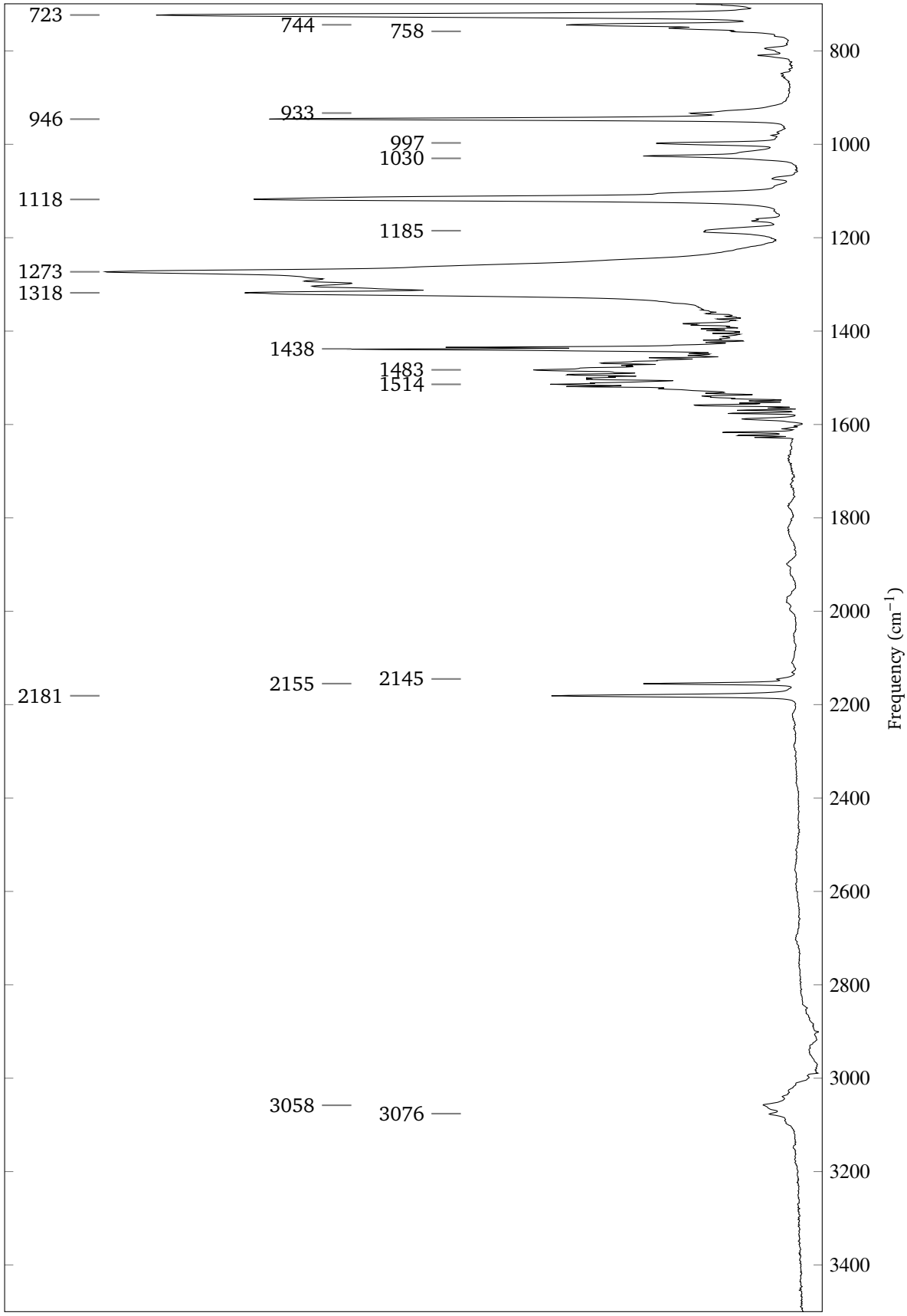

Figure S11: IR Spectrum of Molecular Species **3** With Selected Peaks

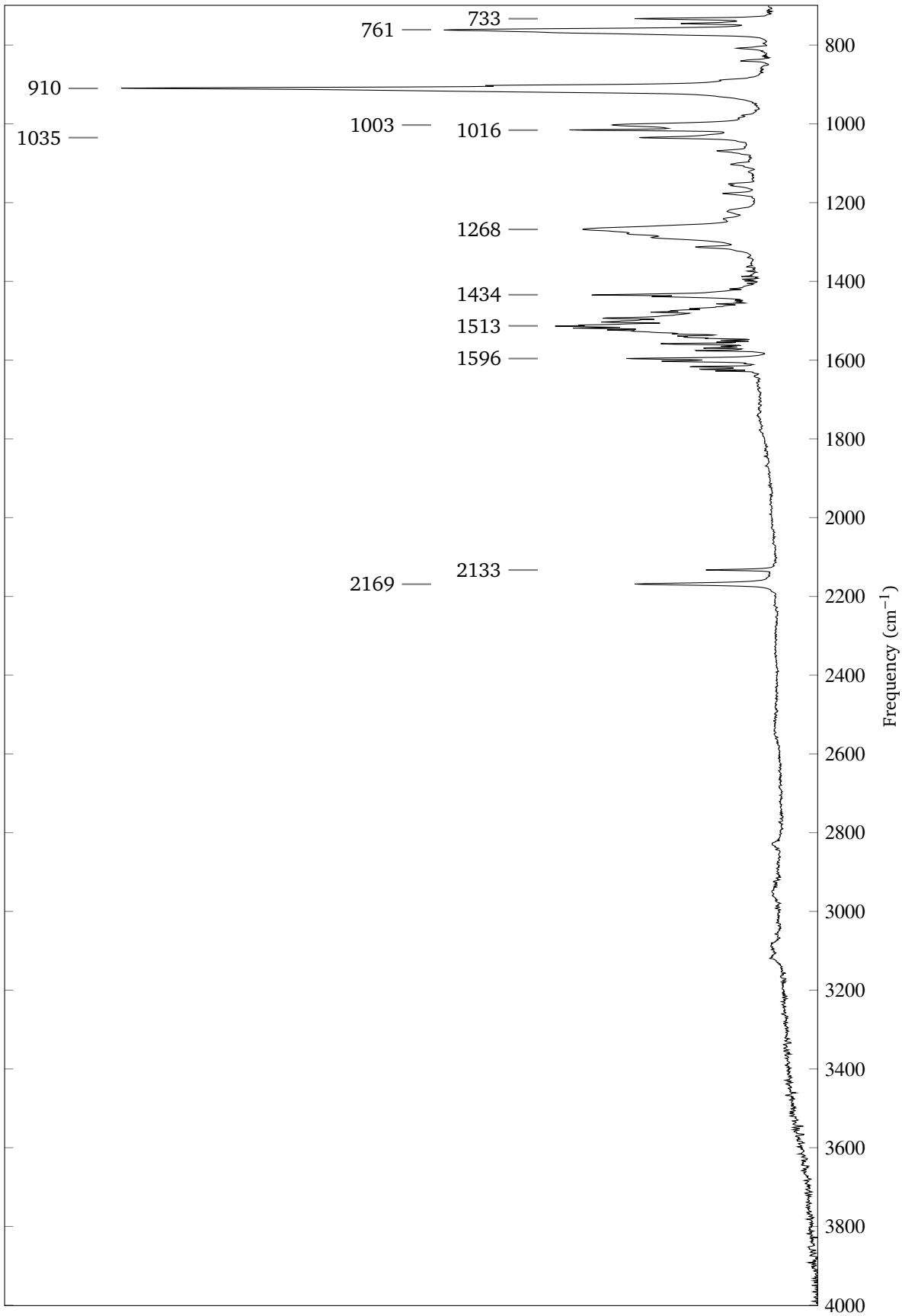

Figure S12: IR Spectrum of bipy Coordination Polymer **4** With Selected Peaks

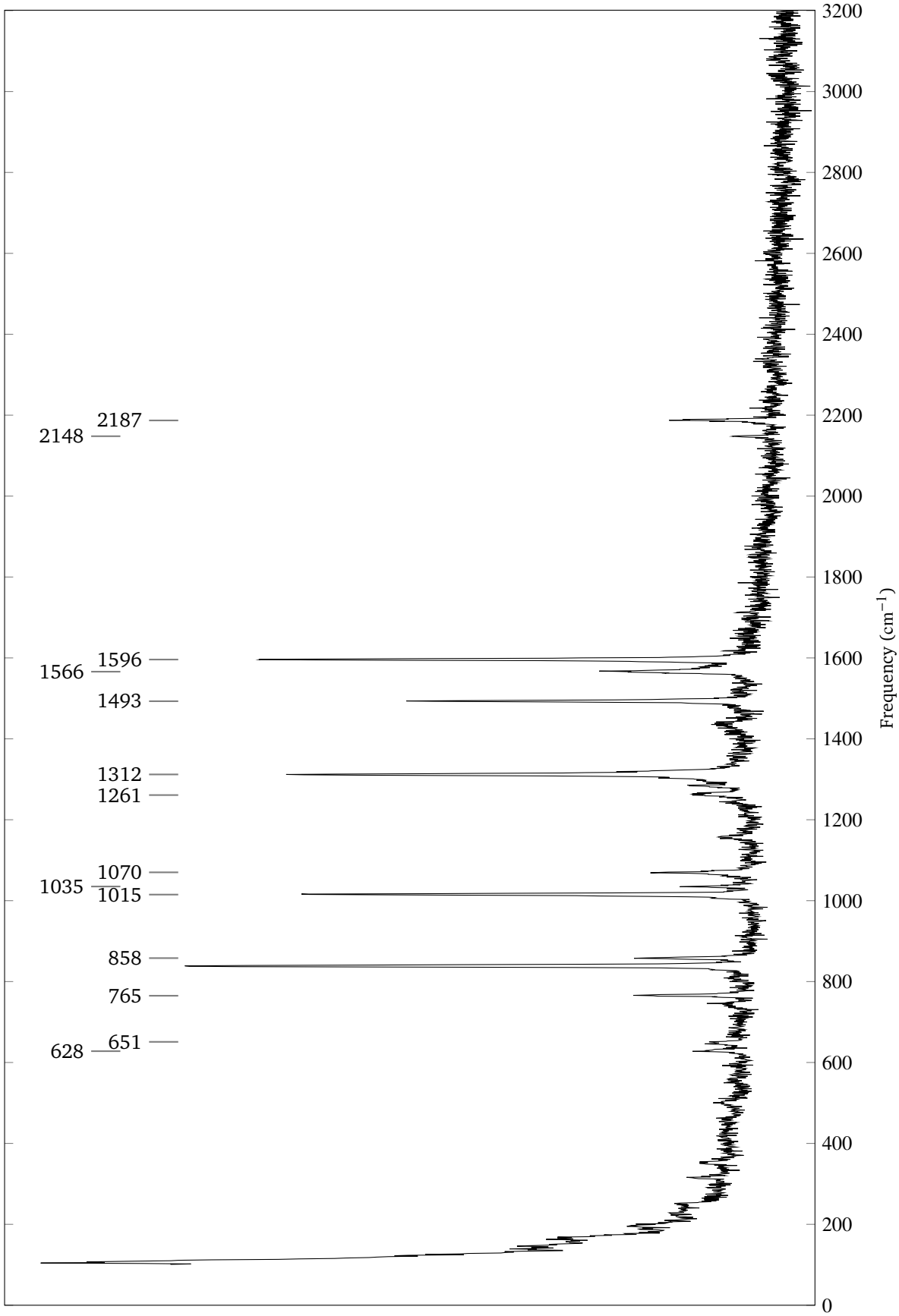

Figure S13: Raman Spectrum of bipy Coordination Polymer **4** With Selected Peaks

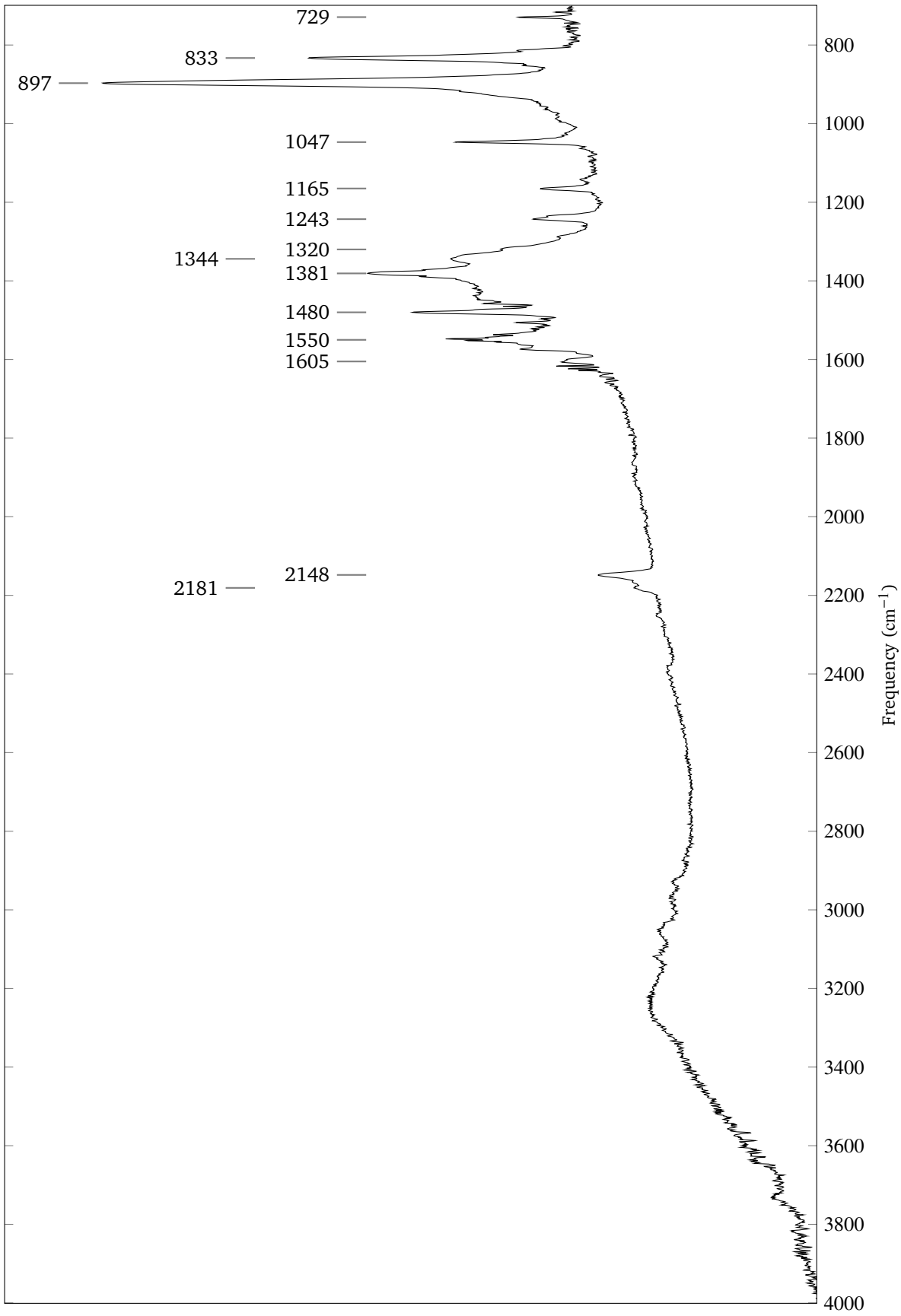

Figure S14: IR Spectrum of Me_2bipy Coordination Polymer **5** With Selected Peaks

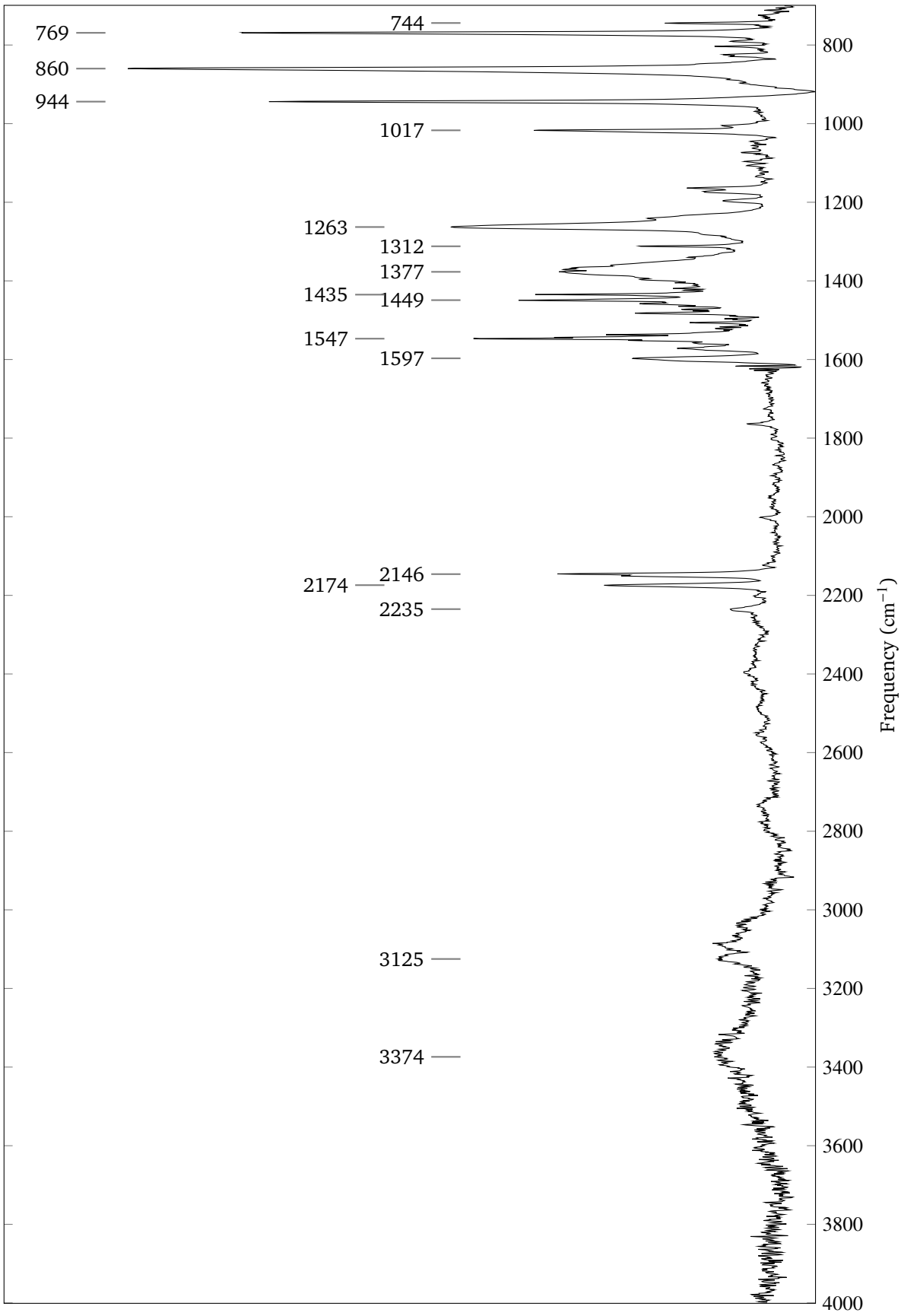

Figure S15: IR Spectrum of Terpy Molecular Species **6** With Selected Peaks

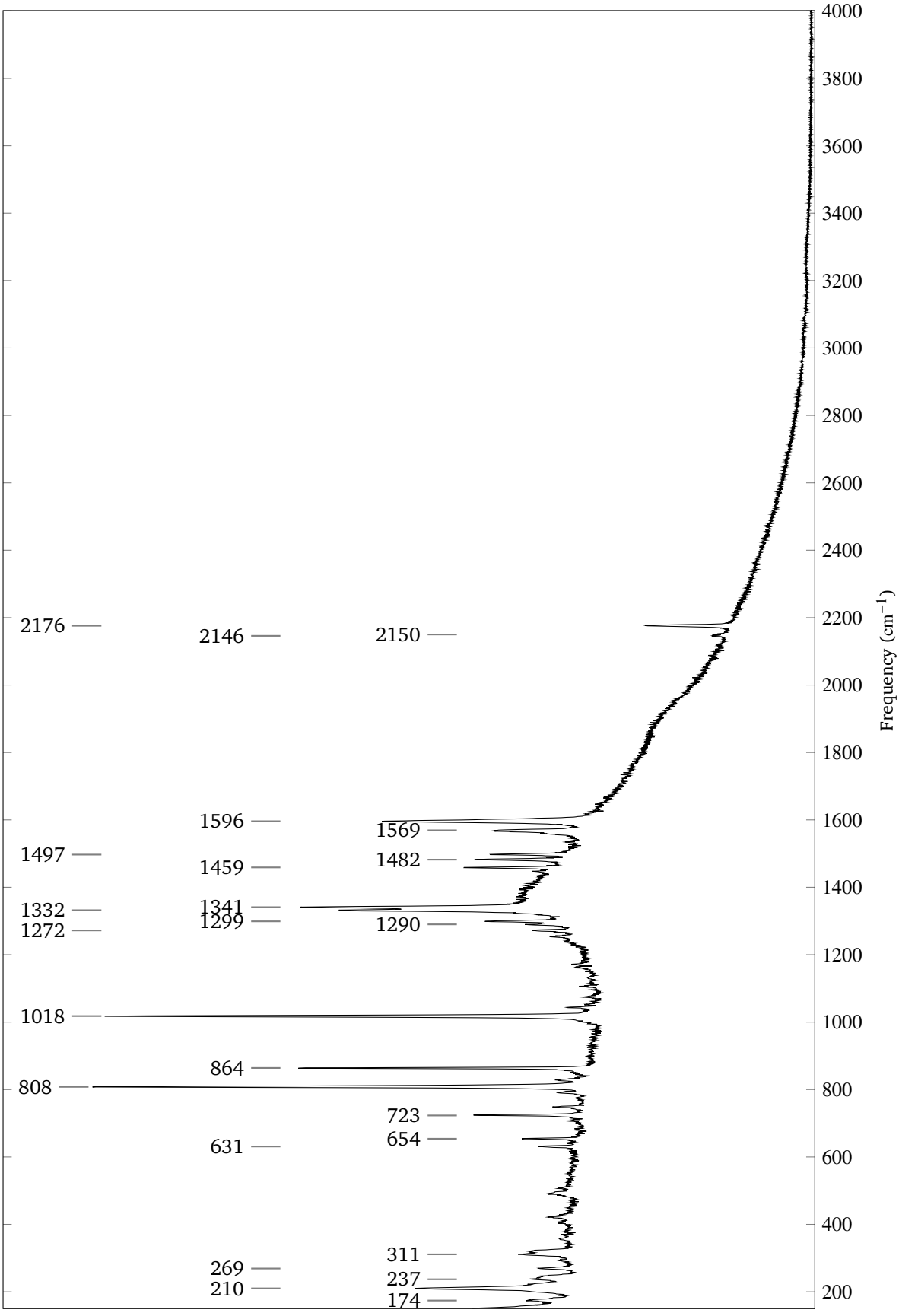

Figure S16: Raman Spectrum of Terpy Compound **6** With Selected Peaks